

Experimental Evidence for a Reduction in Electron Thermal Diffusion due to Trapped Particles

J. A. Reusch,^{1,*} J. K. Anderson,¹ D. J. Den Hartog,^{1,2} F. Ebrahimi,^{1,2} D. D. Schnack,¹ H. D. Stephens,^{1,2} and C. B. Forest^{1,2}

¹*Department of Physics, University of Wisconsin–Madison, 1150 University Avenue, Madison, Wisconsin 53706, USA*

²*Center for Magnetic Self-Organization in Laboratory and Astrophysical Plasmas,
University of Wisconsin–Madison, Madison, Wisconsin 53706, USA*

(Received 20 September 2010; published 6 October 2011)

New high time resolution measurements of the electron thermal diffusion χ_e throughout the sawtooth cycle of the Madison Symmetric Torus reversed-field pinch have been made by utilizing the enhanced capabilities of the upgraded multipoint, multipulse Thomson scattering system. These measurements are compared to the χ_e due to magnetic diffusion predicted by using information from a new high spectral resolution zero- β nonlinear resistive magnetohydrodynamic simulation performed, for the first time, at the Lundquist number of high current Madison Symmetric Torus plasmas ($S \approx 4 \times 10^6$). Agreement between the measured and predicted values is found only if the reduction in thermal diffusion due to trapped particles is taken into account.

DOI: 10.1103/PhysRevLett.107.155002

PACS numbers: 52.55.Hc, 52.25.Fi, 52.65.Kj

Predicting and understanding thermal transport in a stochastic magnetic field is the focus of a great deal of research in both laboratory and astrophysical plasmas [1–6]. In toroidal magnetic confinement devices, overlapping magnetic perturbations can lead to tangled magnetic fields and stochastic transport. In astrophysics, the turbulent motion of the plasma, for example, in galaxy clusters, can generate tangled magnetic fields on vast scales. In their seminal work on the subject, Rechester and Rosenbluth suggest a method for quantifying the stochastic diffusion of the magnetic field lines in laboratory plasmas [2]. More recently, this method has been extended to astrophysical plasmas where an additional reduction in the thermal transport due to trapped particles was suggested [3,7].

The Rechester-Rosenbluth model often predicts thermal transport that is significantly larger than measured in laboratory plasmas [4,6]. One possible explanation for this is that trapped particles, which cannot carry heat along the diffusing field lines out of the system, are generally ignored in this type of analysis. The Madison Symmetric Torus (MST) [8] reversed-field pinch (RFP) is a toroidal magnetic confinement device that is ideally suited for investigating this effect, as the trapped particle fraction is of the order of 50% across much of the minor radius [9], and the magnetic field is stochastic throughout most of the plasma volume [4]. Furthermore, quasiperiodic bursts of MHD activity known as sawteeth cause the degree of stochasticity to vary substantially in both time and space.

In this work, the measured electron thermal diffusion χ_e is compared to the predicted thermal diffusion due to diffusing magnetic field lines, χ_{MD} . χ_{MD} agrees with the measured χ_e only when the reduction in thermal transport due to trapped particles is included in the calculation. With this corrected χ_{MD} , the diffusion of the magnetic field is found to account for all of the measured heat transport in the midradius of the plasma for over half of the sawtooth

cycle. In the core region of the plasma, other transport mechanisms become important before and during the crash while χ_{MD} still slightly overpredicts χ_e after the crash.

A quantitative comparison of χ_e to χ_{MD} throughout the sawtooth cycle is needed in order to gain a complete understanding of the extent to which the thermal diffusion in the RFP is dominated by the diffusion of the magnetic field lines. Significant advances in both the diagnostic capabilities on MST and computer power have enabled the study of the electron thermal diffusion at previously unrealizable levels of confidence. Advances in the Thomson scattering system, in particular, have enabled high time resolution measurements of the thermal diffusion, while advances mainly in computer power have enabled high spectral resolution, nonlinear resistive MHD simulations of the MST plasma at a Lundquist number which, for the first time, matches that of high current standard discharges in MST ($S = \tau_r/\tau_a = a\mu_0 v_a/\eta \approx 4 \times 10^6$, where a is the minor radius, v_a is the Alfvén velocity, and η is the electrical resistivity).

Sawteeth in MST are quasiperiodic global MHD events. The cyclic nature of these events makes them ideal markers in time for ensemble averaging. All of the work presented here from both experiment and simulation represents an ensemble average of sawtooth events. For the experimental data, the ensemble consists of over 5000 sawtooth events which had a plasma current and density within 20% of the target values ($I_p = 400$ kA, $n_e = 1 \times 10^{19}$ m⁻³), although the majority of events were within 10% of those values.

A major advance presented in this work is the determination of the sawtooth evolution of the electron temperature profile at the relatively high time resolution of 20 kHz. The time evolution is found by sorting the temperature data from many shots into time bins relative to the sawtooth time and performing a bin average. By using this method,

the time resolution is effectively limited only by the amount of electron temperature data available. A time resolution of 20 kHz was selected for all of the experimental data shown, as this was the maximum data rate for which all of the radial locations in each time bin contained at least 20 data points. This ensures that the statistics of each bin are sufficient to estimate the uncertainty in the average value, or standard error, as σ/\sqrt{N} , where σ is the standard deviation and N is the number of measurements in the bin. Figure 1 shows the time evolution of the electron temperature for a point near the core and a point near the edge of the MST plasma. T_e in the core decreases slowly leading up to the sawtooth crash, and that heat accumulates in the edge. At the crash, all the magnetic modes resonant inside the plasma grow rapidly, and much of the stored thermal energy in both the core and edge is lost. The core T_e reaches a minimum about 0.25 ms after the crash but then recovers rapidly, while the temperature in the edge reaches a minimum slightly later in time and takes several milliseconds to recover.

Measurement of the T_e profile evolution at high time resolution and low uncertainty coupled with the equilibrium reconstruction code MSTFIT [9] has allowed the sawtooth evolution of χ_e to be determined with a high degree of confidence. The thermal diffusion in MST is found by performing a low resolution fit of the χ_e profile to the electron temperature data via the energy conservation equation which, assuming Fourier's law $q_e = -n_e\chi_e\nabla T_e$ (where q_e is the electron heat flux and n_e is the electron number density), can be written as

$$\frac{\partial}{\partial t} \left(\frac{3}{2} n_e T_e \right) = \frac{1}{\rho} \frac{\partial}{\partial \rho} \left(\rho n_e \chi_e \frac{\partial}{\partial \rho} T_e \right) + \eta J_{\parallel}^2 - \text{sinks}. \quad (1)$$

Here $\rho = \sqrt{V_{\psi}/2\pi^2 R}$ is the effective radial ordinate, as V_{ψ} is the volume of a flux tube and R the major radius of MST. This definition of energy conservation assumes that rapid equilibration along field lines will make the parallel gradient of the heat flux zero. The dominant term at all times is the Ohmic power dissipation, which is approximated as ηJ_{\parallel}^2 , where η is the neoclassical resistivity and J_{\parallel}

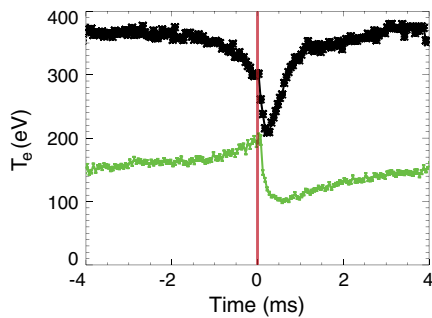


FIG. 1 (color online). Electron temperature versus time for a point near the core (black) and a point near the edge (green) of the plasma. Time $t = 0$ is the sawtooth crash.

is the parallel current density profile calculated at each time point by MSTFIT. Formally, the zeroth order parallel Ohm's law has an additional inductive term, which has been ignored as it is small even at the sawtooth crash. The radiative losses and electron to ion collisional losses are accounted for in the sinks term. Convective transport, which is expected to be negligible except in the edge [10], has been ignored in this work. Formally, Eq. (1) is a partial differential equation, but, by treating $\frac{\partial}{\partial t}(n_e T_e)$ as a known quantity, it becomes an ordinary differential equation and can be solved through a simple matrix inversion. This time derivative of the electron pressure is found to be small except at the sawtooth, where it briefly reaches nearly 50% of the Ohmic dissipation term. Fitting the T_e profile by solving Eq. (1) effectively keeps the choice of model for the electron temperature profile from having a significant impact on the value of χ_e . Instead, there is now a choice of model for the electron thermal diffusion which can often be informed by physical effects expected in the system [11,12]. An uncertainty estimate is made for each of the quantities in Eq. (1) and propagated through the χ_e fit by a Monte Carlo analysis to yield the uncertainty estimate for χ_e shown here. Finally, Z_{eff} was not measured for this data set but is assumed to have a constant value of 3 ± 2 .

Figure 2 shows three fits of the electron thermal diffusion [Fig. 2(a)] and the corresponding electron temperature profiles [Fig. 2(b)] from before, during, and after the sawtooth. The plasma is divided into four regions: the core region where the longest wavelength poloidal mode number $m = 1$ modes are resonant (roughly the inner half of the minor radius), the midradius region where many of the shorter wavelength $m = 1$ modes are resonant, the region in which the $m = 0$ modes are resonant, and an outer region where edge effects are important. The main focus of this work is the two inner regions where the $m = 1$ modes are resonant. The thermal diffusion in these regions, as can be seen in Fig. 2(a), changes by orders of magnitude over the course of the sawtooth cycle.

The time evolution of the heat transport in MST is qualitatively very similar to the evolution of the magnetic mode activity, suggesting that the heat transport is driven by magnetic fluctuations. To perform a quantitative

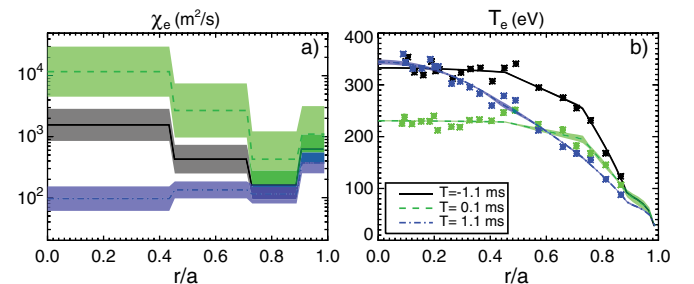


FIG. 2 (color online). Electron thermal diffusion (a) and temperature (b) versus radius at 3 times.

comparison, however, the radial profile of the magnetic fluctuation amplitudes must be determined. These profiles are difficult to measure, so, for this work, they are estimated through simulation.

Simulating the RFP is a computational challenge due to the large number of nonlinearly interacting resonant magnetic perturbations that exist in the plasma. These modes must be properly accounted for, because they make a significant contribution to the evolution of the magnetic equilibrium through the MHD dynamo [13]. Over the course of several decades, advances in both code and computer hardware have enabled the simulation of RFP dynamics at increasingly experimentally relevant parameters. This work presents a new high spectral resolution simulation performed with the DEBS code. This simulation was performed at a Lundquist number that, for the first time in this type of nonlinear simulation of the RFP, matches that of high current discharges in MST, and, as such, some time will be spent discussing them.

The DEBS code is a cylindrical, single fluid, nonlinear, resistive MHD code that can take the resistivity profile, Lundquist number, and current from the experiment as inputs. While this code has undergone many modifications and improvements since it was first introduced, the primary advance that has allowed this work is simply the improvement of computer technology. The simulation presented here uses a force-free equilibrium, so the input resistivity profile, taken from experimental data, was fixed in time for the entire simulation. This means that, while the 3D fluctuations in velocity and magnetic field were self-consistently evolved, pressure-driven effects are absent. Additionally, a high viscosity that was dynamically adjusted to damp subgrid-scale fluctuations was used (see the appendix of Ref. [14]). This effectively keeps the time steps large enough that the long time scale evolution of the system can be studied.

It has long been observed in zero- β simulations that as the Lundquist number is increased, intermittent bursts of MHD activity begin to occur [15]. At experimental values of the Lundquist number, these bursts sharpen and the period between bursts lengthens to match the 6–8 ms period seen in the MST. This simulation was allowed to run for over 15% of a resistive time, generating 23 sawtooth events in the current flattop. This large number of sawteeth has allowed the simulation results to be ensemble-averaged in the same way the experimental data are averaged so that a direct comparison can be made.

A striking feature of both the experiment and the simulation is the change in the safety factor profile $q = rB_z/RB_p$ through the sawtooth. A typical q profile is shown in Fig. 3(a), while Fig. 3(b) shows the time evolution of q at the magnetic axis for the ensemble-averaged simulated data and the experimental data from MSTFIT equilibrium reconstructions. Note that the safety factor in both MST and the simulated plasma decrease as the current

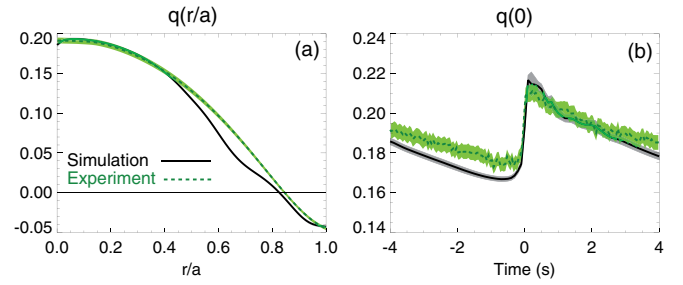


FIG. 3 (color online). Comparison of the ensemble-averaged safety factor (a) versus radius at a time 4 ms before the sawtooth crash and (b) versus time at the magnetic axis.

density is peaked by the Ohmic drive circuit. At the sawtooth crash, q on axis increases and, assuming the axisymmetric approximation for the safety factor holds (see Ref. [16] for a discussion on why this may not be the case), the $m = 1$, $n = 5$ mode becomes resonant inside the plasma. The simulated magnetic field and current density profiles also evolve through a sawtooth in a similar way to the experimental data (not shown).

The magnetic fluctuations in the RFP play a critical role in governing the evolution of the magnetic equilibrium. The simulated mode amplitudes are, on average, about a factor of 2 higher than those measured in MST, though the spectral shape of the modes is very similar to that seen in MST. This discrepancy in mode amplitude has been seen in the past and persists in simulations run at experimental values of the Lundquist number. Work done with the extended MHD code NIMROD suggests that this discrepancy may be because of the lack of two fluid effects, in particular, ion gyroviscosity [17], which DEBS is currently unable to model.

To accurately determine the magnetic diffusion for MST, the ensemble-averaged mode amplitudes from DEBS must be scaled to match the ensemble-averaged mode amplitudes measured at the edge of the experiment. In order to perform this scaling, each ensemble-averaged mode amplitude from DEBS was scaled at each time point to match the ensemble-averaged value for the corresponding mode measured at the edge of MST. By using this set of scale factors, the mode amplitudes at each time step of the simulation can be scaled by determining its time relative to the closest sawtooth. The magnetic field is then traced with the Magnetic Lines (MAL) code [18], and χ_{MD} is then calculated. χ_{MD} is defined as

$$\chi_{MD} = v_{th,e} D_{mag} = v_{th,e} \frac{\langle (r - r_0)^2 \rangle}{2L}, \quad (2)$$

where $v_{th,e}$ is the electron thermal velocity, r is the minor radial position, and L is the distance along the field line. The χ_{MD} profile is ensemble-averaged and compared to the measured χ_e from MST.

An initial comparison of χ_{MD} to the measured χ_e found that χ_{MD} significantly overpredicted the thermal diffusion

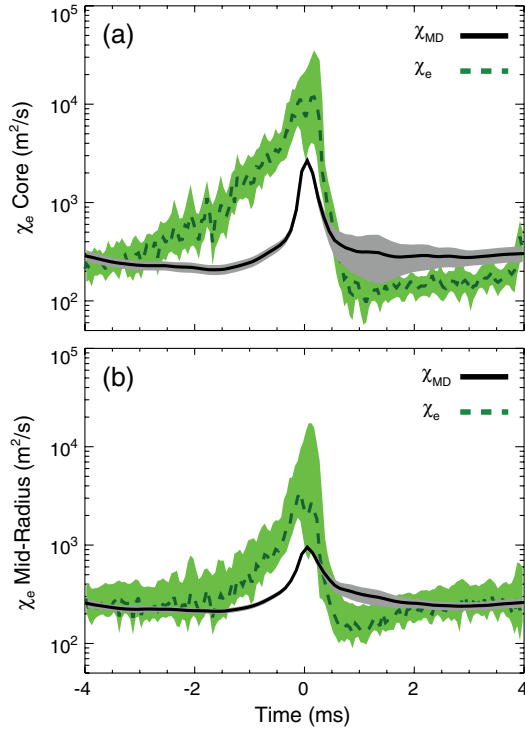


FIG. 4 (color online). Comparison of the average electron thermal diffusion for (a) the core region ($0 \leq r/a \leq 0.45$) and (b) the midradius region ($0.45 \leq r/a \leq 0.7$).

in general. This was unexpected, as χ_{MD} should be the minimum possible value for χ_e . However, as is pointed out in Ref. [3], trapped particles will not conduct heat along magnetic field lines, and, thus, χ_{MD} should be defined as

$$\chi_{MD} = f_c v_{th,e} D_{mag}, \quad (3)$$

where f_c is the circulating fraction of the electron population. The time evolution of the measured electron thermal diffusion is compared to that from Eq. (3) in Fig. 4. With this correction, it becomes clear that the thermal conduction in the midradius is dominated by magnetic diffusion throughout most of the sawtooth cycle. In the core, the magnetic diffusion likely accounts for all of the measured χ_e after the crash, but there are obviously other mechanisms that become important leading up to and including the crash time. These mechanisms may include the presence of magnetic islands [19] [which Eq. (3) will not account for correctly due to the bounded nature of the field lines around the island [18]], as well as nonlinear mechanisms like those described in Ref. [20].

In conclusion, new high time resolution measurements of the electron temperature profile made with the upgraded Thomson scattering system on MST have enabled the study of the sawtooth evolution of the electron thermal diffusion in different regions of the plasma. χ_e is found to vary by nearly 2 orders of magnitude in the core region, peaking at the sawtooth crash and reaching a minimum shortly thereafter. The midradius has a similar time

history, though with a somewhat smaller variation. A new high spectral resolution resistive MHD simulation has been performed, at the Lundquist number of high current discharges in MST, that reproduces many of the characteristics and features of the experiment. By scaling the magnetic eigenmodes from the simulation to the values measured at the edge of MST and tracking the magnetic field line diffusion, a prediction for the electron thermal diffusion was made. While this value should represent a minimum value of χ_e , it generally overestimates the measured value by about a factor of 2 unless the reduction due to trapped particles is taken into account. In MST the trapped fraction is non-negligible, and, once taken into account, the predicted value of diffusion is found to account for all of the measured thermal diffusion in the midradius for slightly more than half of the sawtooth cycle. In the core region, however, the magnetic diffusion accounts for only a fraction of the measured diffusion leading up to the sawtooth crash and slightly overpredicts the measured diffusion after this time.

The authors thank the UW–Madison MST group, including collaborators from UCLA, for their many contributions. This work supported by U.S. DOE Grant No. DE-FC02-05ER54814 and NSF Grant No. PHY 0821899.

*jareusch@wisc.edu

- [1] A. B. Rechester and T. H. Stix, *Phys. Rev. Lett.* **36**, 587 (1976).
- [2] A. B. Rechester and M. N. Rosenbluth, *Phys. Rev. Lett.* **40**, 38 (1978).
- [3] B. D. G. Chandran and S. C. Cowley, *Phys. Rev. Lett.* **80**, 3077 (1998).
- [4] T. M. Biewer, C. B. Forest, J. K. Anderson, G. Fiksel, B. Hudson, S. C. Prager, J. S. Sarff, J. C. Wright, D. L. Brower, W. X. Ding, and S. D. Terry, *Phys. Rev. Lett.* **91**, 045004 (2003).
- [5] A. Baldi, W. Forman, C. Jones, P. Nulsen, L. David, R. Kraft, and A. Simionescu, *Astrophys. J.* **694**, 479 (2009).
- [6] G. Park, C. S. Chang, I. Joseph, and R. A. Moyer, *Phys. Plasmas* **17**, 102503 (2010).
- [7] B. D. G. Chandran, S. C. Cowley, M. Ivanushkina, and R. Sydora, *Astrophys. J.* **525**, 638 (1999).
- [8] R. N. Dexter, D. W. Kerst, T. W. Lovell, S. C. Prager, and J. C. Sprott, *Fusion Technol.* **19**, 131 (1991).
- [9] J. K. Anderson, C. B. Forest, T. M. Biewer, J. S. Sarff, and J. C. Wright, *Nucl. Fusion* **44**, 162 (2004).
- [10] T. M. Biewer, Ph.D. thesis, University of Wisconsin–Madison, 2002.
- [11] L. Frassinetti, A. Alfier, R. Pasqualotto, F. Bonomo, and P. Innocente, *Nucl. Fusion* **48**, 045007 (2008).
- [12] L. Frassinetti, P. Brunzell, M. Cecconello, and J. Drake, *Nucl. Fusion* **49**, 025002 (2009).
- [13] S. Ortolani and D. D. Schnack, *Magnetohydrodynamics of Plasma Relaxation* (World Scientific, Singapore, 1993).
- [14] J. Scheffel and D. Schnack, *Nucl. Fusion* **40**, 1885 (2000).

-
- [15] S. Cappello and D. Biskamp, *Nucl. Fusion* **36**, 571 (1996).
[16] H.D. Stephens, D.J.D. Hartog, C.C. Hegna, and J.A. Reusch, *Phys. Plasmas* **17**, 056115 (2010).
[17] J.R. King, C.R. Sovinec, and V.V. Mirnov, *Phys. Plasmas* **18**, 042303 (2011).
[18] B. Hudson II, Ph.D. thesis, University of Wisconsin–Madison, 2006.
[19] R. Fitzpatrick, *Phys. Plasmas* **2**, 825 (1995).
[20] S.C. Prager, *Plasma Phys. Controlled Fusion* **32**, 903 (1990).